Antarctic Holocene climate change: A benthic foraminiferal stable isotope record from Palmer Deep

Amelia E. Shevenell and James P. Kennett

Department of Geological Sciences and the Marine Science Institute, University of California, Santa Barbara, California, USA

Received 5 October 2000; revised 1 November 2001; accepted 30 November 2001; published 10 May 2002.

[1] The first moderate- to high-resolution Holocene marine stable isotope record from the nearshore Antarctic continental shelf (Ocean Drilling Program (ODP) Hole 1098B) suggests sensitivity of the western Antarctic Peninsula hydrography to westerly wind strength and El Niño-Southern Oscillation (ENSO)-like climate variability. Despite proximity to corrosive Antarctic water masses, sufficient $CaCO_3$ in Palmer Deep sediments exists to provide a high-quality stable isotopic record (especially in the late Holocene). Coherence of benthic foraminifer $\delta^{18}O$, $\delta^{13}C$, sedimentologic, and $CaCO_3$ fluctuations suggests that rapid (<20 years) Palmer Deep bottom water temperature fluctuations of 1°–1.5°C are associated with competitive interactions between two dominant oceanographic/climatic states. An abrupt shift from a warmer, stable Upper Circumpolar Deep Water (UCDW) state to a cooler, variable shelf water state occurred at ~3.6 ka. Palmer Deep bottom waters oscillated between UCDW and shelf water-dominated states between ~3.6 and 0.05 ka. Cool shelf water intervals correlate with Neoglacial events, the most recent and largest being the Little Ice Age (LIA; ~0.7–0.2 ka). Similarities between Palmer Deep and global Holocene records and the rapidity of inferred bottom water fluctuations suggest that western Antarctic Peninsula shelf hydrography has not been controlled by thermohaline reorganizations but by variable strength and/or position of the Southern Hemisphere westerly wind field. We suggest that these atmospheric perturbations may have originated in the low-latitude tropical Pacific. *Index Terms:* 4207 Oceanography: General: Arctic and Antarctic oceanography; 4283 Oceanography: General: Water masses; 4870 Oceanography: Biological and Chemical: Stable isotopes; 9310 Information Related to Geographic Region: Antarctica; *Keywords:* Antarctic paleoceanography, stable isotopes, Holocene, climate change, benthic foraminifera

1. Introduction

[2] Traditionally, the Antarctic climate system has been considered relatively stable and often perceived to act independently of other regions of the globe. Thus research has focused on establishing the phasing of interhemispheric climate variability and mechanisms forcing observed relationships [*Bender et al.*, 1994; *Charles et al.*, 1996; *Bard et al.*, 1997; *Blunier et al.*, 1998; *Steig et al.*, 1998; *Domack and Mayewski*, 1999]. A comparison of Quaternary ice core records from Greenland and the Antarctic Polar Plateau indicates a muted and asynchronous Antarctic response to millennial-scale climate change [*Blunier et al.*, 1998]. These observations are complicated by a near-coastal ice core record from West Antarctica (Taylor Dome) that exhibits millennial-scale variability at the end of the last glacial period similar in magnitude and timing (within current dating resolution) to that observed in Greenland [*Steig et al.*, 1998]. Additional high-resolution Antarctic climate records exhibit similar contrasting regional climate patterns to those observed at Vostok and Taylor Dome, indicating that the Antarctic system may be more sensitive to short-term regional climate fluctuations than originally believed [*Mosley-Thompson et al.*, 1990, 1995; *Kreutz et al.*, 1997]. On shorter timescales, Antarctic ice core $\delta^{18}O$ records suggest that during the Little Ice Age (LIA; ~1400–1900 A.D.), West Antarctica may have warmed while East Antarctica cooled [*Mosley-Thompson et al.*, 1990; *Thompson et al.*, 1994; *Kreutz et al.*, 1997, and references therein]. At present, inverse temperatures between Siple and South Pole Station are observed during periods of increased westerly wind strength [*Mosley-Thompson et al.*, 1990; *Kreutz et al.*, 1997, and references therein]. Chronology issues aside, these records suggest that an improved understanding of regional Antarctic climate sensitivity is critical to our identification of mechanisms forcing decadal- to millennial-scale climate change.

[3] Several hypotheses involving thermohaline and atmospheric circulation change have been invoked to explain the origin and phasing of short-term interhemispheric climate variability. The widely accepted "bipolar seesaw" hypothesis argues that North Atlantic Deep Water (NADW) formation/cessation influences oceanic convection and heat transport to produce an asynchronous interhemispheric climate response [*Broecker*, 1998]. For example, during intervals of NADW formation, Northern Hemisphere high latitudes warm while circum-Antarctic regions cool [*Broecker*, 1998]. Climate modeling studies suggest that variations in warm NADW transport to the Southern Ocean may produce a more regional circum-Antarctic climate response [*Crowley*, 1992; *Mikolajewicz et al.*, 1997; *Steig et al.*, 1998, and references therein]. Although decadal- to millennial-scale climate forcing mechanisms traditionally involve thermohaline reorganization initiated in the North Atlantic, atmospheric circulation changes have also been proposed to account for this variability [*Charles et al.*, 1996; *Ninnemann et al.*, 1999]. One such hypothesis suggests that regional Southern Ocean ventilation changes may result from low- to high-latitude atmospheric teleconnections involving Southern Hemisphere westerly wind field fluctuations [*Klinck and Smith*, 1993; *Charles et al.*, 1996; *Labeyrie et al.*, 1996; *Ninnemann et al.*, 1999]. While most proposed forcing mechanisms predict changes in Southern Ocean hydrography, existing Antarctic paleoclimate and paleoceanographic records have yet to provide a clear picture of decadal- to millennial-scale Southern Ocean variability.

[4] The Southern Ocean is an integral component of the global climate system. Its dynamic large-scale physical oceanographic processes influence both global ocean circulation and carbon cycle

0883-8305/02/2000PA000596

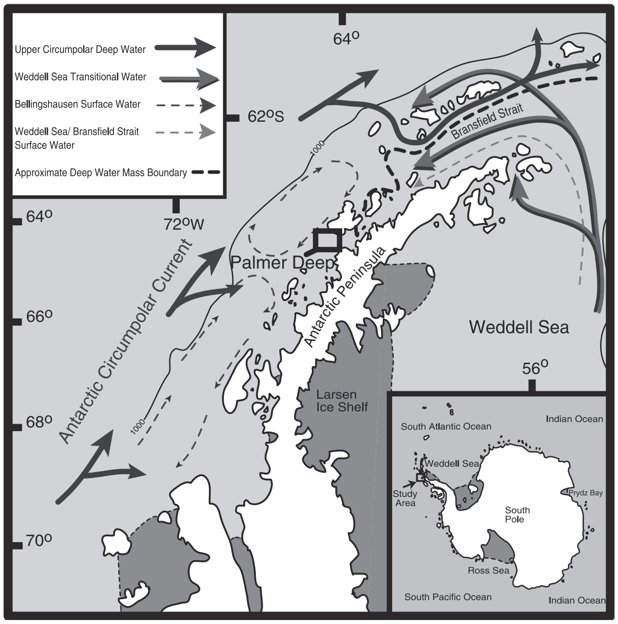

Figure 1. Schematic of oceanographic circulation west of the Antarctic Peninsula (modified from *Hofmann et al.* [1996] and *Ishman and Domack* [1994]). Regional deep water circulation is indicated by solid lines. Surface water circulation is indicated by dashed lines. Arrows suggest general flow direction. Note the location of Palmer Deep. Inset shows Antarctica and the Southern Ocean region.

dynamics in the following ways: (1) the westerly wind-driven Antarctic Circumpolar Current (ACC) integrates Atlantic, Indian, and Pacific Ocean waters; (2) strong upwelling affects oceanic biogeochemistry; and (3) sea ice dynamics influence Antarctic Bottom Water production, deep-ocean ventilation, intermediate and deep ocean circulation, and biologic productivity. These large-scale circum-Antarctic processes must affect regional Southern Ocean hydrography, but understanding of present regional hydrographic variability is limited [*Labeyrie et al.*, 1996]. Thus characterizing regional Antarctic oceanographic/climatic variability at high-resolution is an essential first step in assessing the Southern Ocean's role in global climate change, especially at decadal to millennial timescales.

[5] Marine sedimentary sequences chronicle temporal and spatial oceanographic variability in the Southern Ocean. Southern Ocean sediment records have not yet adequately resolved such fluctuations at high resolution because of problems that include poor calcium carbonate preservation, insufficient dating of recovered sequences, complexities introduced by glacial activity and glacial marine sediments, and regional inaccessibility [*Leventer et al.*, 1993, 1996; *R. C. Smith et al.*, 1999]. Recent efforts have focused on the collection and dating of high-resolution Holocene marine sedimentary sequences from environmentally sensitive Antarctic continental margins, including the western Antarctic Peninsula, Ross Sea, East Antarctic Margin, and Prydz Bay [*Domack et al.*, 1993; *Leventer et al.*, 1993, 1996; *Shevenell et al.*, 1996; *Barcena et al.*, 1998; *Yoon et al.*, 2000; *Domack et al.*, 2001; *Leventer et al.*, 2001].

[6] Characterization of Holocene climate/oceanographic variability in regions of observed environmental sensitivity will improve understanding of natural regional climate dynamics in an era of anticipated anthropogenic climate change [*O'Brien et al.*, 1995; *Keigwin*, 1996; *Leventer et al.*, 1996]. Typically considered a period of relative climatic quiescence, recent globally distributed high-resolution paleoclimate studies identify millennial- to century-scale Holocene climate variability, similar in character, though not in amplitude, to that recorded in the late Pleistocene [*Denton and Karlen*, 1973; *O'Brien et al.*, 1995; *Bond et al.*, 1997]. Significant quasiperiodic (~1500 years) climate events, including the "8.2 ka event" and the LIA, have been documented at both high and low latitudes in the Holocene [*Mosley-Thompson et al.*, 1990; *O'Brien et al.*, 1995; *Keigwin*, 1996; *Bond et al.*, 1997; *Kreutz et al.*, 1997; *Alley et al.*, 1997; *Domack and Mayewski*, 1999; *Crowley*, 2000; *deMenocal et al.*, 2000]. Holocene records from the circum-Antarctic region will provide a more complete picture of Southern Ocean hydrographic variability to advance understanding of the response of the Antarctic system to decadal- to millennial-scale climate change.

[7] The Antarctic Peninsula is the northernmost extension of the Antarctic continent (Figure 1). Its proximity to the Pacific and Atlantic Ocean confluence, the polar/subpolar boundary, and the core of the Southern Hemisphere westerly wind field suggests that the Antarctic Peninsula is ideally situated to record global, zonal, and local atmospheric/hydrographic variability [*Leventer et al.*, 1996; *Shevenell et al.*, 1996; *Domack and Mayewski*, 1999; *R. C. Smith et al.*, 1999]. Significant environmental changes observed along the Antarctic Peninsula since ~1950 (e.g., a ~2.5°C temperature increase, decreasing ice shelf and sea ice extent, and dramatic marine and terrestrial ecosystem changes) indicate that the region may indeed be sensitive to both natural and anthropogenic climate forcing [*Doake and Vaughan*, 1991; *Jones et al.*, 1993; *Domack et al.*, 1995; *Leventer et al.*, 1996; *R. C. Smith et al.*, 1999; *Domack et al.*, 2001]. Ongoing local and regional studies are examining present linkages between physical and biologic processes [*Stammerjohn and Smith*, 1997; *Cunningham and Leventer*, 1998; *Smith et al.*, 1998a, 1998b, 1998c, *D. A. Smith et al.*, 1999, *R. C. Smith et al.*, 1999; *Prezelin et al.*, 2000]. However, these decadal time series studies are still too short to assess natural climate variability and the mechanisms driving this change on decadal to millennial timescales.

[8] The Ocean Drilling Program (ODP) drilled Site 1098 (64°51.7162′S, 64°12.4795′W, 1010 m water depth) in Palmer Deep to obtain a high-deposition rate Holocene sedimentary sequence from the Antarctic continental margin (Figure 2) [*Barker et al.*, 1998]. Here we present the first moderate- to high-resolution Holocene benthic foraminifer stable isotope record from the western Antarctic Peninsula useful for paleoceanographic and paleoclimatic interpretation. Palmer Deep is unique to the Antarctic region because the sequence is adequately dated and contains sufficient $CaCO_3$ to conduct stable isotope studies. Our results document significant decadal- to millennial-scale Holocene paleoceanographic variability in Palmer Deep synchronous with previous lower-resolution sedimentologic studies from the western Antarctic Peninsula, the Ross Sea, and Prydz Bay [*Leventer et al.*, 1993; *Rathburn et al.*, 1997; *Barcena et al.*, 1998; *Kirby et al.*, 1998; *Cunningham et al.*, 1999; *Yoon et al.*, 2000]. Such similarities are important because they suggest regional, not local, Antarctic sensitivity to oceanographic perturbations during the Holocene.

2. Physical Setting

2.1. Palmer Deep

[9] Palmer Deep, a bathymetric depression on the western Antarctic Peninsula continental shelf, consists of two 1000–1400 m deep basins (Basin I and Basin II/III) separated by a 750 m deep sill (Figure 2) [*Barker et al.*, 1998; *Rebesco et al.*, 1998]. Three sedimentary sequences considered in this study (ODP Hole 1098B, and U.S. Antarctic Program (USAP) cores PD92-30 and LMG98-02 KC-1) were collected in ~1000 m water depth from the

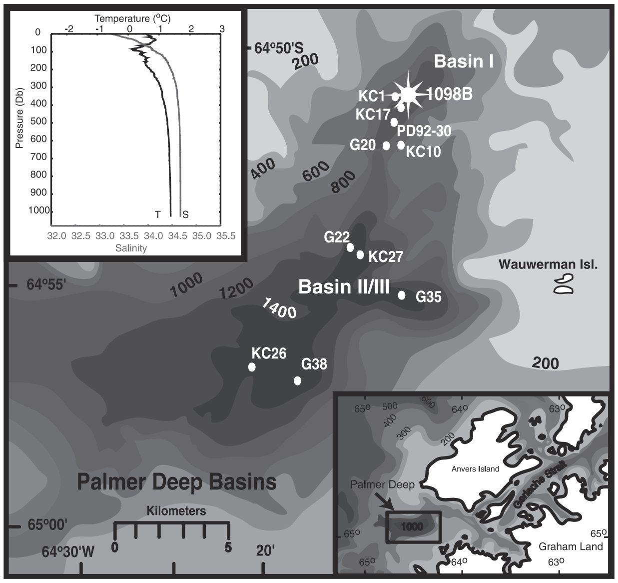

Figure 2. Detailed bathymetry of Palmer Deep with core and grab locations (modified from *Leventer et al.* [1996]). Bottom inset shows coarse regional bathymetry and location of Palmer Deep (modified from *Leventer et al.* [1996]). Top inset shows temperature *T* and salinity *S* profile from Palmer Deep Basin I (taken on USAP cruise LMG98-02; courtesy of E. W. Domack). Note the presence of warm UCDW in Palmer Deep below ~150 m.

southwestern portion of Basin I (Table 1 and Figure 2). Basin I contains 45 m of massive to laminated Holocene diatom ooze and mud with occasional coarse sand and gravel [*Leventer et al.*, 1996; *Barker et al.*, 1998; *Domack et al.*, 1999; *Rebesco et al.*, 1998]. Locally elevated sedimentation rates (~200 cm kyr^{-1} average) result from bathymetric sediment focusing and high regional surface water productivity [*Leventer et al.*, 1996; *Kirby et al.*, 1998; *Rebesco et al.*, 1998].

2.2. Regional Water Masses

[10] Palmer Deep is presently influenced by water from two sources: antarctic intermediate waters derived from the Antarctic Circumpolar Current (ACC) and regionally produced shelf waters [*Hofmann et al.*, 1996; *Hofmann and Klinck*, 1998; *D. A. Smith et al.*, 1999]. Upper Circumpolar Deep Water (UCDW) presently dominates Palmer Deep and western Antarctic Peninsula deep waters (>150 m) (Figure 2) [*Potter and Paren*, 1985; *Hofmann and Klinck*, 1998; *D. A. Smith et al.*, 1999; E. W. Domack, personal communication, 2000]. UCDW is a warm (1°–2°C), saline (34.6–34.7 psu), nutrient-rich, ACC intermediate water mass comprised of recirculated Pacific Ocean, Indian Ocean, and modified NADW waters [*Jacobs et al.*, 1985; *Smith et al.*, 1998a]. The presence of UCDW in Palmer Deep may be related to a combination of the contiguity and strength of the ACC and the proximity of a cross-shelf bathymetric low [*Klinck and Smith*, 1993; *Hofmann and Klinck*, 1998; *Rebesco et al.*, 1998; E. W. Domack, personal communication, 1999]. Modeling work suggests that offshore pressure gradients, similar to those created by northeastward ACC flow along the western Antarctic Peninsula, force upslope flow of UCDW within submarine canyon systems [*Klinck and Smith*, 1993].

[11] The western Antarctic Peninsula shelf is unusual in that its bottom waters generally retain an oceanic character because of the proximity of the ACC's southern boundary (Figure 1) [*Hofmann et al.*, 1996; *D. A. Smith et al.*, 1999]. Regional surface and deep water masses mix with UCDW to create shelf water (cooler and/or fresher UCDW) [*D. A. Smith et al.*, 1999]. Shelf water production likely depends on solar insolation, regional storm severity and frequency, sea ice extent/formation, meltwater production, and Bransfield Strait intermediate water influx (Figure 1) [*Hofmann et al.*, 1996; *D. A. Smith et al.*, 1999]. Palmer Deep surface waters (<150 m) reflect seasonal changes in heat and salt flux resulting from wind forcing, solar insolation, and ice formation/melt [*Hofmann and Klinck*, 1998; *D. A. Smith et al.*, 1999].

2.3. Regional Sea Ice

[12] Sea ice dynamics along the western Antarctic Peninsula may influence regional primary production and sedimentation in Palmer Deep [*Leventer et al.*, 1996; *R. C. Smith et al.*, 1999; *Domack et al.*, 2001]. Therefore consideration of modern sea ice trends and associated forcings is useful for Holocene paleoclimatic and paleoceanographic interpretations. A 20% decline in sea ice coverage has been documented in the southeastern Pacific sector of the Southern Ocean between 1973 and 1993 [*Stammerjohn and Smith*, 1997; *Smith et al.*, 1998c]. This decrease correlates with increased western Antarctic Peninsula surface air temperatures and is antiphased with records of sea ice extent in Pacific, Indian, and Atlantic sectors [*Jacobs and Comiso*, 1993; *Stammerjohn and Smith*, 1997]. On shorter timescales, the southeastern Pacific sector of the Southern Ocean (including the western Antarctic Peninsula) is the only Southern Ocean region to exhibit significant decreases in sea ice extent in phase with El Niño-Southern Oscillation (ENSO) and the related Antarctic Circumpolar Wave (ACW; an eastward propagating disturbance in wind stress, sea ice extent, sea surface temperature, and pressure) [*White and Peterson*, 1996; *Stammerjohn and Smith*, 1997; *R. C. Smith et al.*, 1998c, 1999]. This suggests that the region may exhibit sensitivity to easterly propagating low- to high-latitude atmospheric and oceanic teleconnections [*White and Peterson*, 1996; *Smith et al.*, 1998c]. However, ENSO influences on observed long-term regional climate and oceanographic trends remain unclear.

2.4. Regional Primary Production

[13] The biosilicious nature of the Palmer Deep sedimentary sequence suggests that regional sedimentation is likely controlled by changes in primary production [*Domack et al.*, 1993; *Leventer et al.*, 1996; *Barker et al.*, 1998; *Domack et al.*, 2001]. Southern Ocean primary production has been closely coupled to sea ice extent and oceanic convection [*R. C. Smith et al.*, 1998a, 1998b, 1998c, 1999; *Prezelin et al.*, 2000]. Western Antarctic Peninsula studies suggest that increased springtime regional primary production is associated with sea ice retreat and water column stability, especially during years with increased winter sea ice extent [*Smith et al.*, 1998a, 1998b, 1998c]. Composition of the western Antarctic Peninsula shelf waters has also been shown to affect regional

Table 1. Core Locations, Water Depths, and Lengths

Core	Latitude, °S	Longitude, °W	Water Depth, m	Core Length, m
1098B	64°51.7162′	64°12.4795′	1010	44.7
PD92-30	64°51.720′	64°12.506′	1040	8.8
LMG 98-2 KC-1	64°51.691′	64°13.009′	~1200	1.19

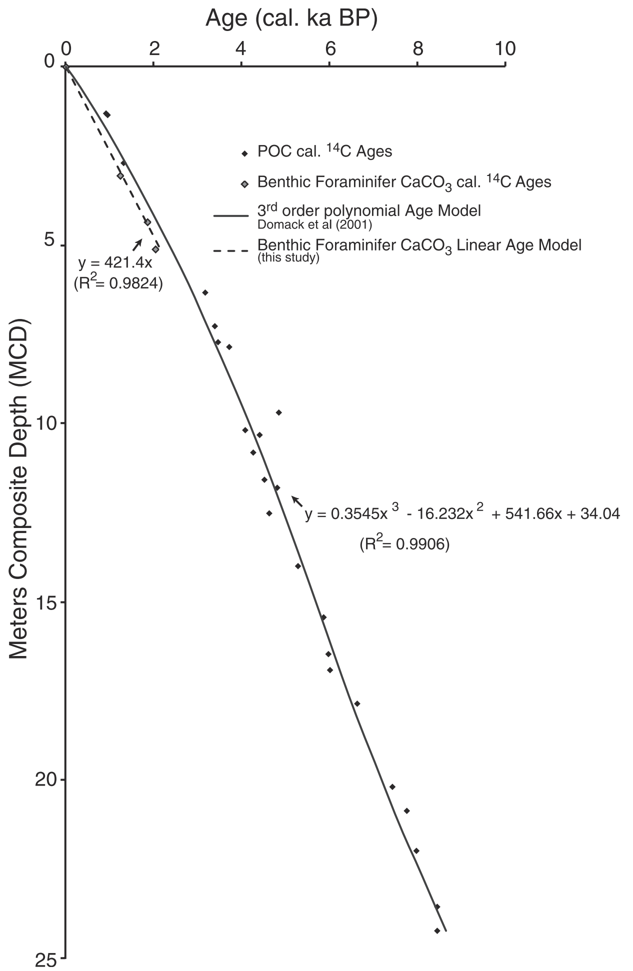

Figure 3. Age versus depth models for Palmer Deep based upon 29 accelerator mass spectrometry (AMS) radiocarbon dates from the upper 25 meters composite depth (mcd). The third-order polynomial age model of *Domack et al.* [2001] is based on both POC and $CaCO_3$ calibrated AMS ^{14}C ages obtained from 0–25 mcd (ODP Hole 1098C and USAP core PD92-30). The linear age model (this study) used between 0 and 5.1 mcd is based on three multispecific benthic foraminifer $CaCO_3$ calibrated AMS ^{14}C dates from USAP core PD92-30. The *Domack et al.* [2001] polynomial age model is used between 5.1 and 25 mcd.

phytoplankton blooms [*Prezelin et al.*, 2000]. UCDW presence along the western Antarctic Peninsula typically corresponds to below average regional sea ice cover [*Stammerjohn and Smith*, 1997; *Hofmann and Klinck*, 1998; *Prezelin et al.*, 2000]. However, upwelled UCDW may provide necessary nutrients to the mixed layer to sustain diatom community dominance during periods of reduced regional sea ice coverage [*Prezelin et al.*, 2000]. Although diatoms are present in all western Antarctic Peninsula coastal regions, diatom-dominated blooms are sustainable only with injection of nutrient-rich UCDW to the photic zone [*Prezelin et al.*, 2000].

3. Chronology

[14] In this study, we employ a modified version of the Palmer Deep age model [*Domack et al.*, 2001]. Our age model is based upon three multispecific benthic foraminifer $CaCO_3$ accelerator mass spectrometry (AMS) ^{14}C dates (USAP core PD92-30) between 0 and 5.1 meters composite depth (mcd) and 21 particulate organic carbon (POC) ^{14}C dates (ODP Hole 1098C) between 5.1 and 25 mcd (Figure 3; all dates are from *Domack et al.* [2001]). Raw radiocarbon dates were calibrated to account for a local reservoir effect of ~1230 years (assumed constant through the sequence [*Domack et al.*, 2001]). Calibrated ages were placed on a mcd scale created for ODP Site 1098 by correlating physical property measurements from ODP Holes 1098A, 1098B, and 1098C [*Acton et al.*, 2001]. Our stable isotope data are from ODP Hole 1098B, PD92-30, and LMG98-02 KC-1. We converted ODP Hole 1098B meters below seafloor (mbsf) depths to the ODP Site 1098 mcd scale following *Acton et al.* [2001]. The ODP Site 1098 mcd scale was applied to USAP cores PD92-30 and LMG98-02 KC-1 by correlating magnetic susceptibility records [*Acton et al.*, 2001; *Domack et al.*, 2001]; cross-correlation suggests that the upper 1.36 m of core PD92-30 are missing [*Domack et al.*, 2001].

[15] *Domack et al.* [2001] obtained an age model for the upper 25 mcd of Palmer Deep using a third-order polynomial regression (Figure 3). In the upper 5.1 mcd of the Palmer Deep sequence, *Domack et al.* [2001] used a combination of POC and multispecific benthic foraminifer $CaCO_3$ AMS ^{14}C dates from 1098C and PD92-30, respectively. Because of ^{14}C dating uncertainties of POC [*Bjorck et al.*, 1991] and the availability of foraminifer $CaCO_3$ ^{14}C dates above 5.1 mcd we chose to use only the three foraminifer $CaCO_3$ ^{14}C dates (2.7, 4.36, and 5.1 mcd [*Domack et al.*, 2001]) to construct a simple linear age model between 0 and 5.1 mcd (Figure 3):

$$y = 421.4x\left(r^2 = 0.98\right),$$

where y is age (calendar years B.P.) and x is depth (mcd). The y intercept was set at 0 calendar years B.P. to account for the 0 calendar year B.P. surface age [*Domack et al.*, 2001]. The resulting linear age-depth profile suggests that sedimentation was continuous at a rate of 240 cm kyr^{-1}, providing a sampling resolution of ~5 yr cm^{-1} for the upper 0–5.1 mcd of the Palmer Deep record (Figure 3). Our linear age model suggests that the *Domack et al.* [2001] polynomial age model overestimates ages in the 0–5.1 mcd interval by ~300 calendar years. We suggest that the observed offset may result from either contamination of POC ^{14}C dates by reworked carbon or that most of the ages contributing to the third-order regression are located deeper in the section (Figure 3). Between 5.1 and 25 mcd the *Domack et al.* [2001] polynomial age model is employed because of the coherence of the POC ^{14}C dates and lack of benthic $CaCO_3$ ^{14}C dates. Sedimentation rates in this interval range between 170 and 340 cm kyr^{-1}, providing a resolution of 3–5 yr cm^{-1} [*Domack et al.*, 2001].

4. Materials/Methods

4.1. Foraminifers

[16] Palmer Deep sediments contain few calcareous foraminifers; planktonic foraminifers are absent from the upper 25 mcd, and calcareous benthic foraminifers (including *Bulimina* spp. and *Bolivina* spp.) are generally only present between 0–8.5 and 29.6–32 mcd (Table 2). Stable isotope measurements (ODP Hole 1098B, PD92-30, KC-1, and grab samples) were conducted on a single benthic foraminifer species, *Bulimina aculeata*. This taxon was chosen for isotopic analysis because of (1) its persistence and abundance through the upper ~9 mcd of the Palmer Deep sedimentary record, (2) its excellent preservation (translucent tests with no visible fragmentation, pitting, or overgrowth), and (3) its tendency to secrete $CaCO_3$ at/near oxygen isotopic equilibrium with the overlying bottom water mass, thus providing reliable bottom water $\delta^{18}O$ records, at least in the temperate latitudes [*McCorkle et al.*, 1990, 1997].

Table 2. Sampling Intervals

Core	Depth Interval, mcd	Sampling Interval, cm	Number of Samples	Average Resolution, years
LMG98-2 KC-1	0–1.15	5	20	~20
1098B	0.115–1.66	1	104	~5
1098B	1.66–1.86	1–5	70	~5–20
PD92-30	1.33–9.63	10	51	~50
1098B	8.6–29.9	5	6	
1098B	29.9–32.7	1–5	17	~3–10

[17] To quantify the relationship between *B. aculeata* $\delta^{18}O$ and the $\delta^{18}O_w$ of subpolar Palmer Deep bottom water, equilibrium calcite $\delta^{18}O$ ($\delta^{18}O_{ec}$) values were calculated following the procedure of *McCorkle et al.* [1990, 1997] (Table 3). Owing to a lack of extensive Palmer Deep $\delta^{18}O_w$ measurements, $\delta^{18}O_w$ values (0 to −0.1‰) were chosen to reflect the UCDW $\delta^{18}O_w$ range in the AP region [*Jacobs et al.*, 1985; *Potter and Paren*, 1985]. Modification of UCDW $\delta^{18}O_w$ on the western AP shelf may result from physical mixing of surface water, meltwater, and regional water masses [*Hofmann and Klinck*, 1998; *Smith et al.*, 1998a]; however, the observed oceanic character of the Palmer Deep bottom water (Figure 2) (E. W. Domack, personal communication, 2000) and minimal present-day regional deep water formation [*D. A. Smith et al.*, 1999] suggest that the present volume of influx would not significantly alter regional $\delta^{18}O_w$ beyond this range. *B. aculeata* oxygen isotopic values from Palmer Deep surface sediment samples (Rose Bengal stained; 0–1 cm depth) appear close to predicted $\delta^{18}O_{ec}$ values for regional bottom waters (Tables 3 and 4). Therefore observed variability in the down core $\delta^{18}O$ signal likely reflects fluctuations in temperature (~1°–1.5 °C) and $\delta^{18}O_w$ composition of Palmer Deep bottom water. Interpretation of the *B. aculeata* $\delta^{13}C$ record is more difficult because of its infaunal habitat [*McCorkle et al.*, 1990]. The benthic foraminifer $\delta^{13}C$ record likely reflects both the influence of respired organic matter and $\delta^{13}C_{DIC}$ of pore waters as well as changes in the bottom water $\delta^{13}C$ [*McCorkle et al.*, 1990; *Mackensen et al.*, 1993; *McCorkle et al.*, 1997; R. Dunbar, personal communication, 2001].

4.2. Stable Isotope Analysis

[18] Initial sampling was conducted at moderate resolution (5–10 cm) from ODP Hole 1098B, PD92-30, and KC-1. Sampling resolution was subsequently increased to 1 cm in intervals containing sufficient carbonate (see Table 2); of these additional samples, ~20% contained insufficient carbonate to conduct isotopic analyses. Sediment samples were prepared for stable isotopic analysis using standard techniques. A small number of specimens (3–12) of *B. aculeata* were picked from the >150 μm fraction, dried, and roasted under vacuum at 350°C for 1 hour prior to analysis to remove organic contaminants. Prepared samples were reacted with orthophosphoric acid at 90°C in an on-line carbonate CO_2 preparation device, and the generated CO_2 was analyzed using a Finnigan/MAT 251 light stable isotope mass spectrometer at the University of California, Santa Barbara. Data are expressed in the standard delta notation (‰) relative to the Peedee belemnite (PDB) carbonate standard through repeat analyses of standard NBS-19. Long-term instrument precision of the standard NBS-19, measured over a period of several years, is <0.09‰ for both $\delta^{18}O$ and $\delta^{13}C$. Stable isotopic data were generated in random order from 286 samples. Duplicate and triplicate analyses of 40 samples from the 0.5–2.0 mcd interval of ODP Hole 1098B and core KC-1 were conducted over a 10 month period to ensure data reproducibility.

Table 3. The $\delta^{18}O$ of Calcite in Equilibrium With Palmer Deep Bottom Water

	Value
Basin I water depth	~1000 m
Temperature, °C (K)[a]	1.48 (274.63)
$\delta^{18}O_w$, ‰ SMOW[b]	−0.05‰
$\delta^{18}O_{ec}$, ‰ PDB[c]	3.45‰

[a] The bottom water temperature value comes from a conductivy-temperature-depth cast taken by *Domack et al.* [1999] in the Palmer Deep (Figure 2).

[b] The $\delta^{18}O_w$ was estimated to range between 0 and −0.1‰ (SMOW) based upon average CDW values [*Jacobs et al.*, 1985; *Potter and Paren*, 1985; *Meredith et al.*, 1999].

[c] The $\delta^{18}O_{ec}$ (‰ SMOW) was calculated using the equation of *O'Neil et al.* [1969] following *McCorkle et al.* [1990]: $10^3 \ln \alpha$ ($CaCO_3$-H_2O) = $2.78 \times 10^6/T^2 - 3.39$. This is rearranged to obtain $\delta^{18}O_{ec}$ (‰ PDB) (following *McCorkle et al.* [1990]): $\delta^{18}O_{ec} = 2.78 \times 10^6/T^2 - 33.0857 + (\delta^{18}O_w - 0.27)$, where T is in °K and $\delta^{18}O_w$ is in SMOW.

5. Results

5.1. Carbonate Distribution

[19] The down hole distribution of Palmer Deep stable isotope data is likely an adequate gauge of $CaCO_3$ presence. Sediments are predominantly biosilicious with generally high total organic carbon accumulation (60–180 mmol cm^{-2} kyr^{-1} (R. Dunbar, personal communication, 2001)) and low wt % $CaCO_3$ (0.3–1.2 % [*Barker et al.*, 1998]) above 30 mcd. Sediment trap data (R. Dunbar, personal communication, 2001) and low sedimentary wt % $CaCO_3$ (typically <1 % [*Barker et al.*, 1998]) indicate that calcareous nannofossils are not regionally abundant. This observation and the lack of preserved planktonic foraminifers suggest that benthic foraminifer $CaCO_3$ is the dominant source of sedimentary $CaCO_3$ in Palmer Deep. Our data distribution indicate that $CaCO_3$ is (1) present between 9.5 and 9.0 ka (32.5–29.6 mcd), (2) absent between 9.0 and 3.6 ka (29.6–8.5 mcd), (3) present during elevated magnetic susceptibility intervals between 3.6 and 0.67 ka (8.5–1.6 mcd), and (4) present between 0.67 and 0.05 ka (1.6–0.12 mcd) (Figure 4).

5.2. Stable Isotope Records

[20] *B. aculeata* oxygen isotope records from ODP Hole 1098B and cores PD92-30 and LMG98-02 KC-1 exhibit a very slight trend toward more negative values up section (Figures 4 and 5). High-amplitude $\delta^{18}O$ variability (<10 year ~0.2–0.3‰ $\delta^{18}O$ shifts) occurs between ~9.5 and 0.67 ka (~32–1.6 mcd) in intervals of elevated magnetic susceptibility (Figures 4 and 5). Continuous $CaCO_3$ presence between 0.67 and 0.05 ka (1.6–0.12 mcd) allowed for production of a late Holocene high-resolution stable isotope record (Figures 5 and 6). Well-resolved low-amplitude $\delta^{18}O$ periodicity is observed between 0.67 and 0.05 ka (1.6–0.12 mcd). Periods of more positive $\delta^{18}O$ are centered at ~0.55, ~0.4, and ~0.25 ka (1.32, 0.94, and 0.59 mcd). Periods of more negative $\delta^{18}O$ are centered at ~0.64, ~0.48, and ~0.33 ka (1.52, 1.14, and 0.78 mcd) (Figure 6).

Table 4. Measured Palmer Deep Core Top $\delta^{18}O$ Values and Offset From Calculated $\delta^{18}O_{ec}$ for a Range of UCDW $\delta^{18}O_w$ Values

Sample	Location	$\delta^{18}O$	$\delta^{18}O - \delta^{18}O_{ec}$ ($\delta^{18}O_w = -0.02$‰ SMOW)
LMG98- G19	Basin I	3.40	−0.08
LMG98- G20	Basin I	3.37	−0.11
KC- 1	Basin I	3.41	−0.07
Basin I Average		3.39	−0.09
LMG98- G22	Basin II	3.34	−0.14
LMG98- KC- 27	Basin II	3.48	0.0
LMG98- G35	Basin II	3.35	−0.13
Basin II Average		3.39	−0.09
LMG98-KC- 26	Basin III	3.40	−0.08
LMG98- G38	Basin III	3.39	−0.09
KC- 17	Basin III	3.35	−0.13
Basin III Average		3.38	−0.07
Total Average		3.39	−0.09

[21] In general, *B. aculeata* $\delta^{13}C$ values are positively correlated with $\delta^{18}O$ values in the Palmer Deep sedimentary sequence (Figures 4–6). $\delta^{13}C$ values are most negative in the ~9.5–9.1 ka (32–30 mcd) interval (Figure 4). Between 3.6 and 0.67 ka (8.5–1.6 mcd), $\delta^{13}C$ values are slightly more positive than in recent sediments (0.67–0.05 ka; 1.6–0.12 mcd), and high-amplitude $\delta^{13}C$ variability exists. Muted low-amplitude $\delta^{13}C$ periodicity exists between 0.67 and 0.05 ka (1.6–0.12 mcd; Figure 6). Periods of more positive $\delta^{13}C$ correlate with more positive $\delta^{18}O$ intervals and more negative $\delta^{13}C$ intervals correlate with more negative $\delta^{18}O$ intervals (Figure 6). Observed $\delta^{13}C$ and $\delta^{18}O$ coherence is consistent with either bottom water $\delta^{13}C_{DIC}$ or biogenic productivity changes, both of which should result from water mass fluctuations.

[22] We compared our stable isotope and inferred $CaCO_3$ records to the more complete magnetic susceptibility record from ODP Hole 1098B [*Barker et al.*, 1998]. Our results confirm the previous observation that biogenic $CaCO_3$ presence generally correlates with relatively high magnetic susceptibility (Figures 4–6) [*Leventer et al.*, 1996]. The most important result of the stable isotope/magnetic susceptibility comparison is that significant visual correlation exists between $\delta^{18}O$, $\delta^{13}C$, magnetic susceptibility, and gamma ray attenuation porosity evaluator (GRAPE) bulk density records in the 0.67–0.05 ka (1.6–0.12 mcd) interval (Figures 5 and 6) [*Barker et al.*, 1998]. More positive $\delta^{18}O$ correlates with enriched $\delta^{13}C$, high magnetic susceptibility, and high GRAPE bulk density values as well as massive clay-rich siliciclastic sediments, coarse-grained magnetic material, and the presence of biogenic carbonate (Figure 6). More negative $\delta^{18}O$ correlates with more depleted $\delta^{13}C$, low magnetic susceptibility, and low GRAPE bulk density values as well as laminated diatomaceous sequences, minimal siliciclastic influx, fine-grained magnetic material, and an absence of biogenic carbonate (Figure 6).

6. Discussion

6.1. Late Holocene Stable Isotope-Sedimentary Relationships: The High-Resolution Record

[23] The late Holocene (0.67–0.05 ka; 1.6–0.12 mcd) high-resolution benthic foraminifer stable isotope record is the most significant result of this study (Figures 5 and 6). Continuous $CaCO_3$ presence through this elevated magnetic susceptibility interval enables production of a very high-resolution (~5 years) stable isotope record. Late Holocene $\delta^{18}O$, $\delta^{13}C$, magnetic susceptibility, and GRAPE bulk density records [*Barker et al.*, 1998] exhibit significant, synchronous decadal- to century-scale oscillations (Figure 6). In this discussion, we evaluate late Holocene stable isotope and magnetic susceptibility relationships in Palmer Deep and then, assuming these relationships persist, make general paleoenvironmental inferences based on trends in magnetic susceptibility, stable isotope, and $CaCO_3$ through the entire Holocene.

[24] Magnetic susceptibility is a physical sedimentary proxy for variable biogenic and siliciclastic sediment supply. In the Palmer Deep sequence, magnetic susceptibility has been used as a regional paleoenvironmental proxy and interpreted to reflect biogenic productivity changes [*Leventer et al.*, 1996; *Kirby et al.*, 1998;

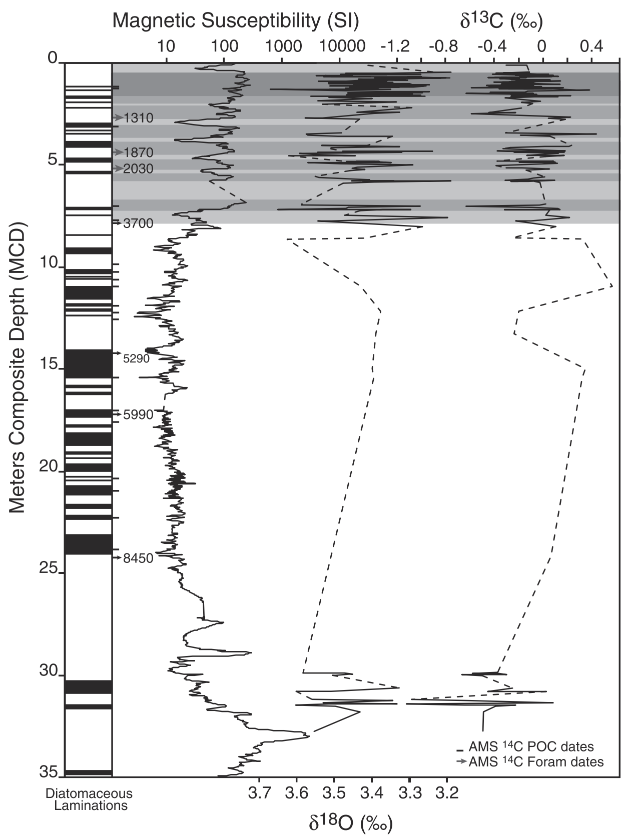

Figure 4. Palmer Deep stable isotope and magnetic susceptibility records [*Barker et al.*, 1998] versus depth (mcd) in ODP Site 1098. Bars indicate the position of AMS ^{14}C dates converted to calendar years before present. Dark bands represent intervals of high diatom concentrations in ODP Hole 1098B [*Barker et al.*, 1998]. Shaded intervals in the graph correspond to high magnetic susceptibility intervals interpreted as intervals of increased shelf water volume in Palmer Deep.

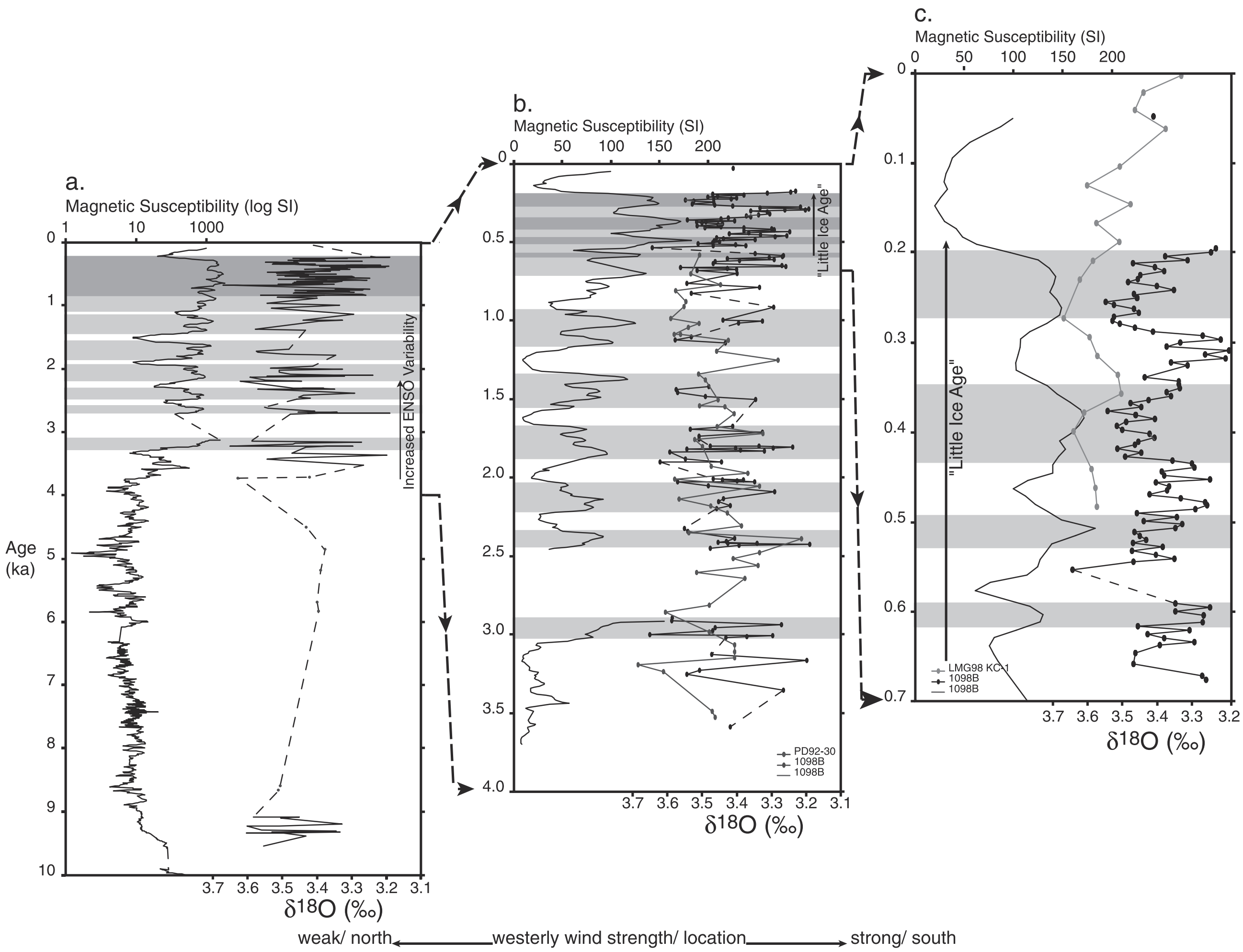

Figure 5. The $\delta^{18}O$ and magnetic susceptibility records from ODP Site 1098 [*Barker et al.*, 1998], Palmer Deep versus age, spanning (a) the last 10 kyr, (b) the last 4 kyr, and (c) the last 0.7 kyr. The PD92–30 $\delta^{18}O$ record is plotted with the ODP Hole 1098B $\delta^{18}O$ record in Figure 5b. The LMG98-02 KC-1 $\delta^{18}O$ record is plotted with the ODP Hole 1098B $\delta^{18}O$ record in Figure 5c. Higher $\delta^{18}O$ and magnetic susceptibility reflect intervals of greater terrigenous influx to Palmer Deep and are interpreted to indicate greater shelf water volume during intervals of increased regional wind strength and/or a southward position of the Southern Hemisphere westerly wind field.

Domack et al., 2001]. Low magnetic susceptibility intervals are interpreted as periods of high biosiliceous productivity during warm, stratified sea surface conditions [*Leventer et al.*, 1996; *Kirby et al.*, 1998; *R. C. Smith et al.*, 1999; *Domack et al.*, 2001]. Regional stabilization of the upper water column results from the presence of low-salinity meltwater and/or thermal warming and may be enhanced during intervals of decreased wind strength [*Leventer et al.*, 1996; *R. C. Smith et al.*, 1999]. Large nutrient-depleting phytoplankton blooms (uncommon in the Southern Ocean) likely occur when stratification restricts cells to the photic zone [*Leventer et al.*, 1996; B. B. Prezelin, personal communication, 2001]. Weak episodic convective or isopycnal mixing events may be sufficient to replenish surface water nutrients and sustain a large bloom event [*R. C. Smith et al.*, 1999; *Prezelin et al.*, 2000]. High magnetic susceptibility intervals represent periods of reduced biogenic productivity associated with increased wind strength resulting in a well-mixed water column [*Leventer et al.*, 1996]. Although surface water nutrients are replenished by deep convective mixing associated with increased wind strength, *Leventer et al.* [1996] argue that deep mixing reduces regional primary productivity by periodically transporting individual cells below the photic zone. Striking similarities between our stable isotope and magnetic susceptibility records strengthen previous assertions that magnetic susceptibility fluctuations reflect paleoceanographic/paleoclimatic variability in Palmer Deep (Figures 5 and 6).

[25] What environmental influences could cause observed stable isotope-sedimentary correlations? We argue that local oceanographic variability (i.e., competitive interactions between cool shelf waters and warm nutrient-rich UCDW) in the basal depths of Palmer Deep can account for the late Holocene stable isotope and sedimentary oscillations. Bottom water instability may result from either fluctuations in the southern boundary of the ACC relative to the western Antarctic Peninsula, variable ACC strength, and/or changes in regional mixing depths that influence regional shelf water production [*Hofmann et al.*, 1996; *Hofmann and Klinck*, 1998; *D. A. Smith et al.*, 1999]. Oceanographic fluctuations along the Antarctic continental margin are notable because of the influence deep shelf waters may exert on regional heat and nutrient fluxes and hence regional sea ice formation and cover, biogenic primary production, and meltwater production (Figure 7) [*Hofmann et al.*, 1996; *D. A. Smith et al.*, 1999]. Our observations indicate significant regional sensitivity to decadal- to millennial-scale oceanographic variability during the Holocene.

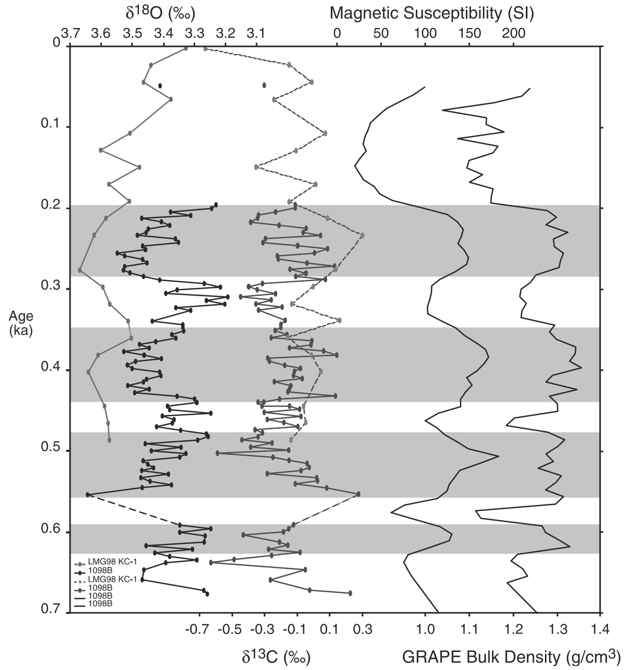

Figure 6. The $\delta^{18}O$, $\delta^{13}C$, magnetic susceptibility, and GRAPE bulk density records from ODP Hole 1098B [*Barker et al.*, 1998] and $\delta^{18}O$ and $\delta^{13}C$ records from LMG98–02 KC-1 versus age spanning the last 0.7 kyr. Higher $\delta^{18}O$, $\delta^{13}C$, magnetic susceptibility, and GRAPE bulk density values reflect intervals of increased shelf water volume in Palmer Deep. Lower $\delta^{18}O$, $\delta^{13}C$, magnetic susceptibility, and GRAPE bulk density values reflect intervals of increased UCDW in Palmer Deep. Hydrographic variability in Palmer Deep is interpreted to reflect changes in the strength and location of the Southern Hemisphere westerly wind field.

[26] During the late Holocene (~0.67–0.05 ka) the continuous presence of $CaCO_3$ and elevated magnetic susceptibility in Palmer Deep reflect a millennial-scale decrease in biologic productivity and increase in colder, fresher, less corrosive regional shelf water production (Figures 6 and 7) [*D. A. Smith et al.*, 1999]. Similar late Holocene trends are observed in low-resolution sedimentary records from the western Antarctic Peninsula [*Domack et al.*, 1993, 1995; *Shevenell et al.*, 1996; *Barcena et al.*, 1998; *Yoon et al.*, 2000]. Low-amplitude stable isotope and sedimentary periodicity through the late Holocene suggests that decadal- to centennial-scale oceanographic oscillations are superimposed on the general shelf water trend (Figures 5 and 6). Intervals of increased cool shelf water volume and/or decreased UCDW volume in Palmer Deep reflect decreased regional productivity and increased terrigenous influx [*Leventer et al.*, 1996; *Domack et al.*, 2001]. During warm nutrient-rich UCDW-dominated intervals in Palmer Deep, biosiliceous primary productivity increases, and terrigenous influx decreases [*Leventer et al.*, 1996; *Domack et al.*, 2001; N. R. Warner and E. W. Domack, Millenial to decadal scale paleoenvironmental change during the Holocene in the Palmer Deep, Antarctica as recorded by particle size analysis, submitted to *Paleoceanography*, 2001 (hereinafter referred to as Warner and Domack, submitted manuscript, 2001)]. This inference is further supported by recent observations from the western Antarctic Peninsula shelf suggesting that diatom productivity is greatest during periods of increased UCDW presence [*Prezelin et al.*, 2000]. Similar decadal- to century-scale fluctuations are observed in records of atmospheric variability from Siple Dome ice core and have been associated with increased regional wind strength related to a deep regional low-pressure cell (Amundsen Sea Low [*Kreutz et al.*, 1997]).

6.2. Long-Term Holocene Record

[27] Below 1.6 mcd, low and variable sedimentary $CaCO_3$ contents limit our ability to obtain or interpret a continuous Holocene stable isotope stratigraphy from Palmer Deep. To better understand paleoceanographic variability in Palmer Deep through the Holocene, we infer that observed late Holocene stable isotope and magnetic susceptibility relationships apply to the ~9.0–0.67 ka (~29–1.6 mcd) interval (Figures 4 and 5). Minimal $CaCO_3$ presence, low magnetic susceptibility values, and diatomaceous laminations in the ~9.0–3.6 ka (~29–8.5 mcd) interval may reflect increased UCDW volume and primary productivity in

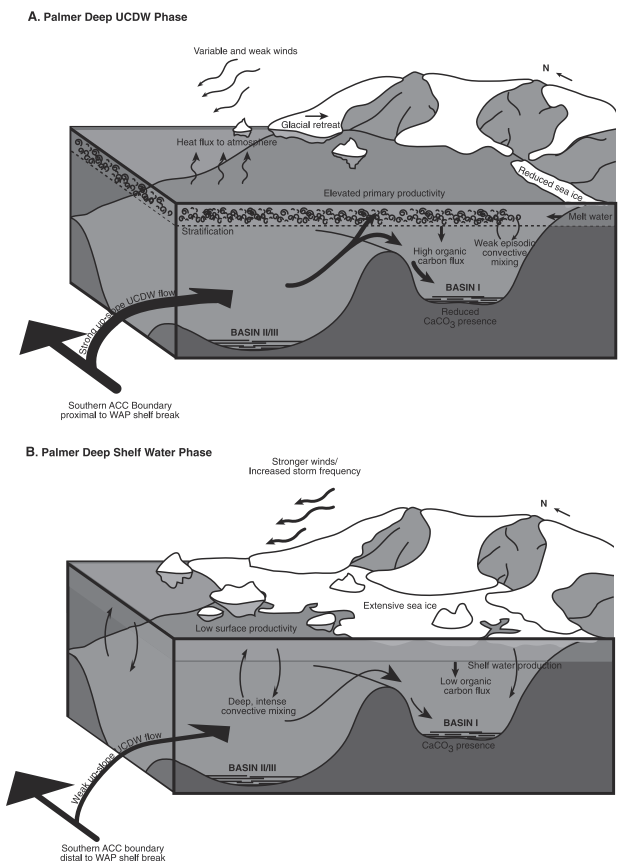

Figure 7. Schematic diagrams of factors influencing Palmer Deep sedimentation. (a) Increased UCDW volume in Palmer Deep reflects weak and variable Southern Hemisphere westerly wind strength and/or a more northerly position of this wind field. The southern boundary of the ACC is more proximal to the western Antarctic Peninsula shelf break. Heat released to the atmosphere from warm UCDW melts regional sea ice, resulting in intense regional stratification and high diatom primary production. (b) Increased shelf water volume in Palmer Deep reflects strong Southern Hemisphere westerly wind strength and/or a more southerly location of this wind field. The southern boundary of the ACC is distal to the western Antarctic Peninsula shelf break, and UCDW volume is reduced in Palmer Deep. Strong regional winds result in deep convective mixing of surface waters with warmer deep waters to create cooler shelf waters. These cooler shelf waters are less corrosive to $CaCO_3$. Increased sea ice extent and a well-mixed water column result in decreased regional primary productivity.

Palmer Deep [*Leventer et al.*, 1996; *Taylor and Sjunneskog*, 2002]. UCDW is an old, corrosive water mass that limits $CaCO_3$ presence on the western Antarctic Peninsula continental shelf; this corrosivity is likely further enhanced by increased local productivity [*Mackensen et al.*, 1993]. We propose that sustained UCDW influence resulted in warmer regional atmospheric and sea surface temperatures, decreased sea ice cover, water column stratification, and increased primary productivity between ~9 and 3.6 ka (Figure 7; ~29–8.5 mcd). This interval corresponds to a general period of decreased Southern Ocean (Pacific sector) meridional wind strength and West Antarctic sea ice extent [*Stager and Mayewski*, 1997].

[28] High-amplitude magnetic susceptibility fluctuations and increased $CaCO_3$ presence beginning at ~3.6 ka (~8.5 mcd) suggest an abrupt shift from a sustained UCDW state to a more variable, less biologically productive state in Palmer Deep. Lower-resolution sedimentary and geochemical studies from the western Antarctic Peninsula region exhibit similar declines in surface productivity [*Domack et al.*, 1993; *Shevenell et al.*, 1996; *Barcena et al.*, 1998; *Yoon et al.*, 2000]. Between ~3.6 and 0.67 ka (~8.5–1.6 mcd), centennial- to millennial-scale magnetic susceptibility and $CaCO_3$ trends suggest that Palmer Deep bottom waters oscillated between UCDW- and shelf water-dominated states. These oscillations have a ~200 year periodicity and may be related to increased wind strength and enhanced vertical mixing or extreme water column stratification, respectively [*Leventer et al.*, 1996; *Domack et al.*, 2001; Warner and Domack, submitted manuscript, 2001]. During shelf water-dominated intervals, stable isotope values show no distinct trends except that the highest amplitude stable isotope variability corresponds with the initial magnetic susceptibility high at ~3.6–2.9 ka (8.5–6.9 mcd). Shelf water intervals correlate with Northern Hemisphere "Neoglacial" events, the most recent and largest being the Little Ice Age (~0.7–0.2 ka [*Denton and Karlen*, 1973; *Wigley and Kelly*, 1990; *Bond et al.*, 1999]). However, because sparse sampling in this interval is limited to conditions that preserve $CaCO_3$ (i.e., intervals of increased shelf water volume/atmospheric circulation), interpretation of the ~9–0.67 ka (29–1.6 mcd) stable isotope record is tentative.

6.3. Forcing Mechanisms

[29] What mechanisms could force the Holocene oceanographic variability observed in Palmer Deep? The western Antarctic Peninsula is situated within the zone of strongest Southern Hemisphere westerly winds [*Kreutz et al.*, 1997, and references within]. We suggest that Palmer Deep stable isotope and sedimentary records document both short- and long-term Holocene westerly wind variability. Similarities between Palmer Deep, West Antarctic [*Kreutz et al.*, 1997; *Stager and Mayewski*, 1997], and global Holocene records [*Dunbar et al.*, 1994; *Cook et al.*, 1995; *Sandweiss et al.*, 1996; *Stager and Mayewski*, 1997; *Black et al.*, 1999; *Rodbell et al.*, 1999; *Haug et al.*, 2001] as well as the rapidity of inferred bottom water fluctuations suggest that western Antarctic Peninsula shelf hydrography is controlled by atmospheric variability and not by thermohaline reorganizations influencing UCDW upwelling. Sensitivity of western Antarctic Peninsula physical processes, such as sea ice extent, to low- to high-latitude atmospheric teleconnections (i.e., ENSO/ACW) also provides compelling evidence for atmospheric forcing of Palmer Deep hydrographic fluctuations [*White and Peterson*, 1996; *Stammerjohn and Smith*, 1997; *Smith et al.*, 1998c].

[30] Westerly wind variability may influence proportions of UCDW and shelf water in Palmer Deep (Figure 7) [*Hofmann et al.*, 1996; *Hofmann and Klinck*, 1998; *D. A. Smith et al.*, 1999]. Late Holocene stable isotope and magnetic susceptibility oscillations exhibit long- and short-term trends similar to atmospheric variability recorded at Siple Dome [*Kreutz et al.*, 1997]. Siple Dome sea salt concentrations document an abrupt increase in wind strength at ~0.6 ka; decadal- to century-scale variability is also observed within the ~0.6–0 ka record [*Kreutz et al.*, 1997]. Strong regional westerly winds correlate with increased shelf water and/or decreased UCDW volume in Palmer Deep. Increased shelf water production during periods of increased atmospheric circulation may result from efficient mixing of surface waters through the water column (Figure 7) [*Leventer et al.*, 1993, 1996; *D. A. Smith et al.*, 1999]. Predominantly offshore winds may also push the southern boundary of the ACC off the western Antarctic Peninsula continental shelf, resulting in a further decrease in the volume of UCDW in Palmer Deep [*Hofmann et al.*, 1996; *D. A. Smith et al.*, 1999]. Intervals of increased UCDW volume in Palmer Deep correlate with less intense westerly winds (reduced Siple Dome sea salt concentrations) [*Kreutz et al.*, 1997]. Decreased wind strength is likely associated with intense water column stratification and elevated biologic productivity due to increased UCDW volume and sea ice meltwater (Figure 7) [*Leventer et al.*, 1996; *Kreutz et al.*, 1997]. Increased UCDW volume may result from a proximal location of the southern boundary of the ACC to the western Antarctic Peninsula continental shelf [*Hofmann et al.*, 1996; *D. A. Smith et al.*, 1999].

[31] Because of present age control limitations the most that may be inferred from our Late Holocene LIA interval (~0.67–0.05 ka [*Grove*, 1988]) is that westerly winds intensified [*Kreutz et al.*, 1997] and Palmer Deep bottom waters cooled (assuming shelf water formation processes similar to today [*D. A. Smith et al.*, 1999]). The suggestion by *Broecker et al.* [1999] that Southern Ocean ventilation may have decreased after the LIA is intriguing and seems consistent with our late Holocene evidence for increased shelf water presence between 0.67 and 0.05 ka and the inferred UCDW increase since ~0.05 ka (Figure 4b). This hypothesis deserves further study when an improved age model is available.

[32] Assuming late Holocene correlations between stable isotope and sedimentary evidence and regional atmospheric circulation records persist for intervals of minimal isotopic data, Palmer Deep may record decadal- to millennial-scale westerly wind variability throughout the Holocene. Periodic (~200 years) oceanographic fluctuations have been observed in the Palmer Deep magnetic susceptibility record and Bransfield Strait diatom records between ~3.6 and 1.0 ka [*Leventer et al.*, 1996; *Barcena et al.*, 1998]. Although this ~200 year periodicity has been attributed to tidal forcing and solar variability [*Leventer et al.*, 1996; Warner and Domack, submitted manuscript, 2001], we suggest this periodicity may be directly linked with westerly wind fluctuations [*Kreutz et al.*, 1997]. An inferred increase in Palmer Deep UCDW volume (~9–3.6 ka) corresponds to decreased wind strength at Taylor Dome between ~8 and 5.5 ka [*Stager and Mayewski*, 1997]. The general increase in Palmer Deep shelf water volume at ~3.6 ka corresponds with high-amplitude westerly wind variability at Taylor Dome; however, Palmer Deep appears insensitive to the initial Taylor Dome wind strength increase at ~5.5 ka [*Stager and Mayewski*, 1997]. Uncertainties associated with the Palmer Deep radiocarbon reservoir correction might account for this observed lag [*Domack et al.*, 2001].

6.4. Global Similarities

[33] Possible supporting evidence for atmospheric forcing of Palmer Deep hydrographic fluctuations comes from low-latitude paleoclimate records [*Dunbar et al.*, 1994; *Cook et al.*, 1995; *Sandweiss et al.*, 1996; *Stager and Mayewski*, 1997; *Black et al.*, 1999; *Rodbell et al.*, 1999; *Haug et al.*, 2001]. We propose that the location and strength of the Southern Hemisphere westerly wind field may be related to atmospheric and oceanographic perturbations generated at lower latitudes [*Sandweiss et al.*, 1996; *Black*

et al., 1999; *Rodbell et al.*, 1999; *Haug et al.*, 2001]. Low- to high-latitude teleconnections are presently recognized in ENSO-sea ice relationships in the western Antarctic Peninsula region [*White and Peterson*, 1996; *Stammerjohn and Smith*, 1997; *Smith et al.*, 1998c] as well as in long-term climate change records.

[34] The Palmer Deep sequence exhibits a significant shift in sedimentary character at ~3.8 ka coincident with a general increase in low-latitude climate variability [*Sandweiss et al.*, 1996; *Baker et al.*, 2000; *Rodbell et al.*, 1999; *Haug et al.*, 2001]. A distinct shift in the character of the Cariaco Basin and Lake Titicaca sequences at ~3.8 ka reflects a southward shift in the location of the Intertropical Convergence Zone (ITCZ) during the Holocene linked to changes in insolation seasonality and ENSO prevalence [*Baker et al.*, 2000; *Haug et al.*, 2001]. Sedimentary and geo-archeological evidence from Peru also imply an increase in the spectral character of ENSO between ~3.5 and 2.6 ka [*Sandweiss et al.*, 1996; *Rodbell et al.*, 1999].

[35] On shorter timescales, our latest Holocene (0.7–0 ka) $\delta^{18}O$ record exhibits fluctuations concurrent with those observed in high-resolution low-latitude coral and marine microfossil sequences [*Dunbar et al.*, 1994; *Black et al.*, 1999]. Late Holocene (~0.8–0 ka) centennial-scale variability in Cariaco Basin may reflect local/regional wind strength fluctuations and/or a more southern ITCZ position [*Black et al.*, 1999]. A change in the Palmer Deep sedimentary character at ~0.7 ka is consistent with this increased low-latitude climate variability [*Black et al.*, 1999] as well as with an increase in the spectral character of ENSO [*Dunbar et al.*, 1994; *Rodbell et al.*, 1999]. Furthermore, centennial oceanographic fluctuations in Palmer Deep correspond to climatic trends observed in Cariaco Basin, western Pacific SST temperatures, and tree ring records from Tasmania, especially between 0.45 and 0.2 ka [*Dunbar et al.*, 1994; *Cook et al.*, 1995; *Black et al.*, 1999].

[36] Although we cannot be certain that Holocene oceanographic variability observed in Palmer Deep is the result of changes in the Southern Hemisphere westerly wind field, lower-latitude records exhibit pronounced high-frequency variability between ~0.7 and 0 ka as well as ~4 and 2.4 ka [*Cook et al.*, 1995; *Baker et al.*, 2000; *Rodbell et al.*, 1999; *Haug et al.*, 2001] similar to that observed in Palmer Deep (within present dating resolution). The apparent synchrony of events in the Palmer Deep and the low-latitudes suggests that Late Holocene climate change may have been initiated in the low latitudes. These similarities in timing and record character suggest that a southern ITCZ position and decreased zonal and meridional atmospheric circulation (ENSO) may result in a southward migration of the Southern Hemisphere westerly wind field [*Labeyrie et al.*, 1996].

7. Conclusions

[37] We present sedimentary and geochemical evidence for Holocene oceanographic fluctuations along the western Antarctic Peninsula. Our results are significant because they document pronounced millennial- to decadal-scale Southern Ocean variability during the Holocene that likely affected regional Antarctic climate regimes. Our late Holocene (0.67–0.05 ka) benthic stable isotope stratigraphy from Palmer Deep represents the first high-resolution record of its kind from the Antarctic marginal marine setting (Figures 5 and 6). Our results demonstrate the following.

1. The late Holocene (0.67–0.05 ka) was a period of enhanced $CaCO_3$ preservation in Palmer Deep. During this interval of inferred regional shelf water production, stable isotope and sedimentary records exhibit pronounced decadal- to century-scale changes attributed to oceanographic variability (Figures 5 and 6). These oceanographic fluctuations may be related to regional westerly wind variability previously associated with a general deepening of the Amundsen Sea Low [*Kreutz et al.*, 1997]. This interval coincides with the LIA, within our present dating resolution.

2. Sedimentary $CaCO_3$ presence corresponds with low biologic productivity and elevated magnetic susceptibility (Figures 4 and 5) [*Leventer et al.*, 1996]. This correlation may be related to the relative proportions of corrosive oceanic UCDW and less corrosive locally derived shelf water in Palmer Deep. Between ~3.6 and 0.67 ka, the Palmer Deep record exhibits strong century-scale (~200 years) oceanographic variability, suggesting oscillations between UCDW- and shelf water-dominated states (Figure 5) [*Leventer et al.*, 1996; *Domack et al.*, 2001]. Similarities between our record and other regional sedimentary and ice core records suggest that long-term oceanographic fluctuations may be driven by variable atmospheric circulation during the Holocene.

3. Strong present-day low- to high-latitude teleconnections (i.e., sea ice variability related to propagation of the ACW) in the western Antarctic Peninsula region indicate that observed century-scale variability in the late Holocene may be associated with high-frequency ENSO variability [*Dunbar et al.*, 1994; *White and Peterson*, 1996; *Stammerjohn and Smith*, 1997; *Smith et al.*, 1998c]. If observed sedimentary and geochemical relationships persist in intervals where $CaCO_3$ is not preserved, the Palmer Deep sedimentary record may record westerly wind variability related to Holocene ENSO dynamics. Our results indicate that oceanographic perturbations in Palmer Deep are generally synchronous with Holocene climate records from West Antarctica as well as with lower latitude records [*Dunbar et al.*, 1994; *Cook et al.*, 1995; *Sandweiss et al.*, 1996; *Kreutz et al.*, 1997; *Stager and Mayewski*, 1997; *Black et al.*, 1999; *Rodbell et al.*, 1999; *Haug et al.*, 2001]. Decreased westerly wind strength may have resulted in a general UCDW increase in Palmer Deep between ~9 and 3.6 ka. A southward migration of westerly winds associated with a southern shift in the low latitude ITCZ [*Baker et al.*, 2000; *Haug et al.*, 2001] and an increase in ENSO strength and variability at ~3.6 ka [*Sandweiss et al.*, 1996; *Rodbell et al.*, 1999] may have resulted in a general increase in Palmer Deep shelf water presence between ~3.6 and 0.05 ka.

[38] We suggest that tropical Pacific climate instability may be transmitted to the high southern latitudes of the Pacific Sector of the Southern Ocean via changes in the strength and location of the Southern Hemisphere westerly wind field [*Labeyrie et al.*, 1996; *Clement et al.*, 1999]. This atmospheric connection suggests synchronous climate forcing between low- and high-latitudes of the Southern Hemisphere. However, regional climate responses to atmospheric forcing are likely to vary throughout the Antarctic [*Kreutz et al.*, 1997]. This work, coupled with observations of rapid warming of the western Antarctic Peninsula region since ~1950 [*Jones et al.*, 1993], illustrates the need for an improved understanding of regional Southern Ocean and Antarctic climate dynamics, especially as related to millennial-scale climate variability and anticipated anthropogenic climate change.

[39] **Acknowledgments.** We thank K. Thompson and H. Berg for technical assistance. We thank S. Brachfeld, E. Domack, R. Dunbar, A. Leventer, and the rest of the Palmer Deep "gang" for helpful dialogues and support. We thank M. Sperling for picking initial *B. aculeata* specimens from ODP Hole 1098B and core top samples. We thank E. Domack for his generosity in providing the PD92-30 and KC-1 samples and CTD data collected on cruise LMG98-02. We thank K. Cannariato, I. Hendy, D. Lea, and U. Ninnemann for insightful discussions during manuscript preparation. We thank L. Peterson and an anonymous reviewer whose comments significantly improved the content and quality of this manuscript. We also acknowledge the ODP Leg 178 Shipboard Scientific Party. Samples from ODP Site 1098 were provided by the Ocean Drilling Program with sponsorship by NSF. This work was supported by a JOI/USSAP grant 178-F000886 to J.P.K.

References

Acton, G. D., C. J. Borton, and the Leg 178 Scientific Party, Palmer Deep composite depth scales for Leg 178 Sites 1098 and 1099, *Ocean Drill. Program Sci. Results*, *178*, 2001. (Available at http://www-odp.tamu.edu/publications/178_SR/chap_05/chap_05.htm)

Alley, R. B., P. A. Mayewski, T. Sowers, M. Stuvier, K. Taylor, and P. U. Clark, Holocene climate instability: A prominent, widespread event 8200 yr ago, *Geology*, *25*, 483–486, 1997.

Baker, P. A., G. O. Seltzer, S. C. Fritz, R. B. Dunbar, M. J. Grove, P. M. Tapia, S. L. Cross, H. D. Rowe, and J. P. Broda, The history of South American tropical precipitation for the past 25,000 years, *Science*, *291*, 640–643, 2000.

Barcena, M. A., R. Gersonde, S. Ledesma, J. Fabres, A. M. Calafat, M. Canals, J. Sierro, and J. A. Flores, Record of Holocene glacial oscillations in Bransfield Basin as revealed by siliceous microfossil assemblages, *Antarct. Sci.*, *10*, 259–285, 1998.

Bard, E., F. Rostek, and C. Sonzogni, Interhemispheric synchrony of the last deglaciation inferred from alkenone palaeothermometry, *Nature*, *385*, 707–710, 1997.

Barker, P. F., et al., *Proceedings of the Ocean Drilling Program, Initial Reports*, vol. 178, Ocean Drill. Program, College Station, Tex., 1998.

Bender, M., T. Sowers, M. L. Dickson, J. Orchardo, P. M. Grootes, P. A. Mayewski, and D. A. Meese, Climate correlations between Greenland and Antarctica during the past 100,000 years, *Nature*, *372*, 663–666, 1994.

Bjorck, S., C. Hjort, O. Ingolfsson, and G. Skog, Radiocarbon dates from the Antarctic Peninsula region—Problems and potential, *Quat. Proc.*, *1*, 55–65, 1991.

Black, D. E., L. C. Peterson, J. T. Overpeck, A. Kaplan, M. N. Evans, and M. Kashgarian, Eight centuries of North Atlantic atmosphere variability, *Science*, *286*, 1709–1712, 1999.

Blunier, T., et al., Asynchrony of Antarctic and Greenland climate during the last glacial, *Nature*, *394*, 739–743, 1998.

Bond, G., W. Showers, M. Cheseby, R. Lotti, P. Almasi, P. deMenocal, P. Priore, H. Cullen, I. Hajdas, and G. Bonani, A pervasive millennial-scale cycle in North Atlantic Holocene and glacial climates, *Science*, *278*, 1257–1266, 1997.

Bond, G. C., W. Showers, M. Elliot, M. Evans, R. Lotti, I. Hajdas, G. Bonani, and S. Johnson, The North Atlantic's 1-2 kyr climate rhythm: Relation to Heinrich Events, Dansgaard/Oeschger Cycles and the Little Ice Age, in *Mechanisms of Global Climate Change at Millennial Time Scales*, *Geophys. Monogr. Ser.*, vol. 112, edited by P. U. Clark, R. S. Webb and L. D. Keigwin, pp. 99–112, AGU, Washington, D. C., 1999.

Broecker, W. S., Paleocean circulation during the last glaciation: A bipolar seesaw?, *Paleoceanography*, *13*, 119–121, 1998.

Broecker, W. S., S. Sutherland, and T. H. Peng, A possible 20th century slowdown of Southern Ocean deep water formation, *Science*, *286*, 1132–1135, 1999.

Charles, C. D., J. Lynch-Stieglitz, U. S. Ninnemann, and R. G. Fairbanks, Climate connections between the hemispheres revealed by deep sea sediment core/ice core correlations, *Earth Planet. Sci. Lett.*, *142*, 19–27, 1996.

Clement, A. C., R. Seager, and M. A. Cane, Orbital controls on the El Niño/Southern Oscillation and the tropical climate, *Paleoceanography*, *14*, 441–456, 1999.

Cook, E., B. M. Buckey, and R. D. D'Arrigo, Interdecadal temperature oscillations in the Southern Hemisphere: Evidence from Tasmanian tree rings since 300 B.C., in *Natural Climate Variability on Decade-to-CenturyTtime Scales*, pp. 532–532, Natl. Acad. Press, Washington, D. C., 1995.

Crowley, T. J., North Atlantic deep water cools the Southern Hemisphere, *Paleoceanography*, *7*, 489–497, 1992.

Crowley, T. J., Causes of climate change over the past 1000 years, *Science*, *289*, 270–277, 2000.

Cunningham, W. L., and A. Leventer, Diatom assemblages in surface sediments of the Ross Sea: Relationship to present oceanographic conditions, *Antarct. Sci.*, *10*, 134–146, 1998.

Cunningham, W. L., A. Leventer, J. T. Andrews, A. E. Jennings, and K. J. Licht, Late Pleistocene-Holocene marine conditions in the Ross Sea, Antarctica: Evidence from the diatom record, *Holocene*, *9*, 129–139, 1999.

deMenocal, P., J. Oritz, T. Guilderson, and M. Sarnthein, Coherent high- and low-latitude climate variability during the Holocene Warm Period, *Science*, *288*, 2198–2202, 2000.

Denton, G. H., and W. Karlen, Holocene climate variations: Their pattern and possible cause, *Quat. Res.*, *3*, 155–203, 1973.

Doake, C. S., and D. G. Vaughan, Rapid disintegration of the Wordie Ice Shelf in response to atmospheric warming, *Nature*, *350*, 328–330, 1991.

Domack, E. W., and P. A. Mayewski, Bi-polar ocean linkages: Evidence from late-Holocene Antarctic marine and Greenland ice-core records, *Holocene*, *9*, 247–251, 1999.

Domack, E. W., T. A. Mashiotta, L. A. Burkley, and S. E. Ishman, 300-year cyclicity in organic matter preservation in Antarctic fjord sediments, in *The Antarctic Paleoenvironment: A Perspective on Global Change*, *Antarct. Res. Ser.*, vol. 60, edited by J. P. Kennett and D. Warnke, pp. 265–272, AGU, Washington, D. C., 1993.

Domack, E. W., S. E. Ishman, A. B. Stein, C. E. McClennen, and A. J. T. Jull, Late Holocene advance of the Muller Ice Shelf, Antarctic Peninsula: Sedimentological, geochemical and paleontological evidence, *Antarct. Sci.*, *7*, 159–170, 1995.

Domack, E. W., et al., Holocene paleoenvironmental change along the Antarctic Peninsula: A test of the solar/bi-polar signal, *LMG98-02 Post-cruise Rep.*, U.S. Antarct. Program, Natl. Sci. Found., Washington, D. C., 1999.

Domack, E. W., A. Leventer, R. Dunbar, F. Taylor, S. Brachfeld, and C. Sjunneskog, Chronology of the Palmer Deep site, Antarctic Peninsula: A Holocene paleoenvironmental reference for the circum-Antarctic, *Holocene*, *11*, 1–9, 2001.

Dunbar, R. B., G. M. Wellington, M. W. Colgan, and P. W. Glynn, Eastern Pacific sea surface temperature since 1600 A.D.: The $\delta^{18}O$ record of climate variability in Galapagos corals, *Paleoceanography*, *9*, 291–315, 1994.

Grove, G. M., *The Little Ice Age*, Cambridge Univ. Press, New York, 1988.

Haug, G. H., K. A. Hughen, D. M. Sigman, L. C. Peterson, and U. Röhl, Southward migration of the Intertropical Convergence Zone through the Holocene, *Science*, *293*, 1304–1308, 2001.

Hofmann, E. E., and J. M. Klinck, Thermohaline variability of the waters overlying the West Antarctic Peninsula continental shelf, in *Ocean, Ice, and Atmosphere: Interactions at the Antarctic Continental Margin*, *Antarct. Res. Ser.*, vol. 75, edited by S. S. Jacobs, pp. 67–81, AGU, Washington, D. C., 1998.

Hofmann, E., E. Klinck, J. M. Lascara, C. M., and D. A. Smith, Water mass distribution and circulation west of the Antarctic Peninsula and including Bransfield Strait, in *Foundations for Ecological Research West of the Antarctic Peninsula*, *Antarct. Res. Ser.*, vol. 70, edited by R. M. Ross and L. B. Quetin, pp. 61–80, AGU, Washington, D. C., 1996.

Ishman, S. E., and E. W. Domack, Oceanographic controls on benthic foraminifers from the Bellingshausen margin of the Antarctic Peninsula, *Mar. Micropaleontol.*, *24*, 119–155, 1994.

Jacobs, S. S., and J. C. Comiso, A recent sea-ice retreat west of the Antarctic Peninsula, *Geophys. Res. Lett.*, *20*, 1171–1174, 1993.

Jacobs, S. S., R. G. Fairbanks, and Y. Horibe, Origin and evolution of water masses near the Antarctic continental margin: Evidence from $H_2{}^{18}O/H_2{}^{16}O$/ ratio in seawater, in *Oceanology of the Antarctic Continental Shelf*, *Antarct. Res. Ser.*, vol. 43, edited by S. S. Jacobs, pp. 59–85, AGU, Washington, D. C., 1985.

Jones, P. D., R. Marsh, T. M. L. Wigley, and D. A. Peel, Decadal timescale links between Antarctic Peninsula ice core oxygen-18 and temperature, *Holocene*, *3*, 14–26, 1993.

Keigwin, L. D., The Little Ice Age and Medieval Warm Period in the Sargasso Sea, *Science*, *274*, 1504–1508, 1996.

Kirby, M. E., E. W. Domack, and C. E. McClennen, Magnetic stratigraphy and sedimentology of Holocene glacial marine deposits in the Palmer Deep, Bellingshausen Sea, Antarctica: Implications for climate change?, *Mar. Geol.*, *152*, 247–259, 1998.

Klinck, J. M., and D. A. Smith, Effect of wind changes during the Last Glacial Maximum on the circulation of the Southern Ocean, *Paleoceanography*, *8*, 427–433, 1993.

Kreutz, K. J., P. A. Mayewski, L. D. Meeker, M. S. Twickler, S. I. Whitlow, and I. I. Pitalwala, Bipolar changes in atmospheric circulation during the Little Ice Age, *Science*, *277*, 1294–1296, 1997.

Labeyrie, L., et al., Hydrographic changes of the Southern Ocean (southeast Indian sector) over the last 230 kyr, *Paleoceanography*, *11*, 57–76, 1996.

Leventer, A., R. B. Dunbar, and D. J. DeMaster, Diatom evidence for late Holocene climatic events in Granite Harbor, Antarctica, *Paleoceanography*, *8*, 373–386, 1993.

Leventer, A., E. W. Domack, S. E. Ishman, S. Brachfeld, C. E. McClennen, and P. Manley, Productivity cycles of 200–300 years in the Antarctic Peninsula region: Understanding linkages among the Sun, atmosphere, oceans, sea ice and biota, *Geol. Soc. Am. Bull.*, *108*, 1626–1644, 1996.

Leventer, A., S. Brachfeld, E. Domack, R. Dunbar, P. Manley, and the Shipboard Scientific Party, Coring Holocene Antarctic Ocean sediments, *NBP01-01 post-cruise rep.*, U.S. Antarctic Program, Natl. Sci. Found., Washington, D. C., 2001.

Mackensen, A., D. K. Futterer, H. Grobe, and G. Schmiedl, Benthic foraminiferal assemblages from the eastern South Atlantic Polar Front region between 35° and 57°S: Distribution, ecology, and fossilization potential, *Mar. Micropaleontol.*, *22*, 33–69, 1993.

McCorkle, D. C., L. D. Keigwin, B. H. Corliss, and S. R. Emerson, The influence of microhabitats on the carbon isotopic composition of deep-sea benthic foraminifera, *Paleoceanography*, *5*, 161–185, 1990.
McCorkle, D. C., B. H. Corliss, and C. A. Farnham, Vertical distributions and stable isotopic compositions of live (stained) benthic foraminifera from the North Carolina and California continental margins, *Deep Sea Res., Part I*, *44*, 983–1024, 1997.
Meredith, M. P., K. E. Grose, E. L. McDonagh, K. J. Heywood, R. D. Frew, and P. F. Dennis, Distribution of oxygen isotopes in the water masses of Drake Passage and the South Atlantic, *J. Geophys. Res.*, *104*, 20,949–20,962, 1999.
Mikolajewicz, U. J., T. J. Crowley, A. Schiller, and R. Voss, Modeling North Atlantic/North Pacific teleconnections during the Younger Dryas, *Nature*, *387*, 384–387, 1997.
Mosley-Thompson, E., L. G. Thompson, P. M. Grootes, and N. Gundestrup, Little Ice Age (Neoglacial) paleoenvironmental at Siple Station, Antarctica, *Ann. Glaciol.*, *14*, 199–204, 1990.
Mosley-Thompson, E., L. G. Thompson, J. F. Paskievitch, M. Pourchet, A. J. Gow, M. E. Davis, and J. Kleinman, South Pole snow accumulation has increased in recent decades, *Ann. Glaciol.*, *21*, 131–138, 1995.
Ninnemann, U. S., C. D. Charles, and D. A. Hodell, Origin of global millennial-scale climate events: Constraints from the Southern Ocean deep sea sedimentary record, in *Mechanisms of Global Climate Change at Millennial Time Scales*, *Geophys. Monogr. Ser.*, vol. 112, edited by P. U. Clark, R. S. Webb, and L. D. Keigwin, pp. 99–112, AGU, Washington, D. C., 1999.
O'Brien, S. R., P. A. Mayewski, L. D. Meeker, D. A. Meese, M. S. Twickler, and S. I. Whitlow, Complexity of Holocene climate as reconstructed from a Greenland ice core, *Science*, *270*, 1962–1964, 1995.
O'Neil, J. R., R. N. Clayton, and T. K. Mayeda, Oxygen isotope fractionation in divalent metal carbonates, *J. Chem. Phys.*, *51*, 5547–5558, 1969.
Potter, J. R., and J. G. Paren, Interaction between ice shelf and ocean in George VI Sound, Antarctica, in *Oceanology of the Antarctic Continental Shelf*, *Antarct. Res. Ser.*, vol. 43, edited by S. S. Jacobs, pp. 35–58, AGU, Washington, D. C., 1985.
Prezelin, B. B., E. Hofmann, C. Mengelt, and J. M. Klink, The linkage between Upper Circumpolar Deep Water (UCDW) and phytoplankton assemblages on the West Antaractic Peninsula continental shelf, *J. Mar. Res.*, *58*, 165–202, 2000.
Rathburn, A. E., J. J. Pichon, M. A. Ayress, and P. De Deckker, Microfossil and stable-isotope evidence for changes in Late Holocene palaeoproductivity and palaeoceanographic conditions in the Prydz Bay region of Antarctica, *Palaeogeogr. Palaeoclimatol. Palaeoecol.*, *131*, 485–510, 1997.
Rebesco, M., A. Camerlenghi, L. De Santis, E. Domack, and M. Kirby, Seismic stratigraphy of Palmer Deep: A fault bounded late Quaternary sediment trap on the inner continental shelf, Antarctic Peninsula Pacific margin, *Mar. Geol.*, *151*, 89–110, 1998.
Rodbell, D. T., G. O. Seltzer, D. M. Anderson, M. B. Abbott, D. B. Enfield, and J. H. Newman, An ~15,000-year record of El Nino-driven alluviation in southwestern Ecuador, *Science*, *283*, 516–520, 1999.
Sandweiss, D. H., J. B. Richardson, E. J. Reitz, H. B. Rollins, and K. A. Maasch, Geoarcheological evidence from Peru for a 5000 year B.P. onset of El Nino, *Science*, *273*, 1531–1533, 1996.
Shevenell, A. E., E. W. Domack, and G. Kernan, Record of Holocene paleoclimate change along the Antarctic Peninsula: Evidence from glacial marine sediments, Lallemand Fjord, in *Climate Succession and Glacial Record of the Southern Hemisphere*, edited by M. R. Banks and M. J. Brown, *Pap. Proc. R. Soc. Tasmania*, *130*, 55–64, 1996.
Smith, D. A., E. E. Hofmann, J. M. Klinck, and C. M. Lascara, Hydrography and circulation of the West Antarctic Peninsula continental shelf, *Deep Sea Res., Part I*, *46*, 925–949, 1999.
Smith, R. C., K. S. Baker, M. L. Byers, and S. E. Stammerjohn, Primary productivity of the Palmer Long Term Ecological Research Area and the Southern Ocean, *J. Mar. Syst.*, *17*, 245–259, 1998a.
Smith, R. C., K. S. Baker, and M. Vernet, Seasonal and interannual variability of phytoplankton biomass west of the Antarctic Peninsula, *J. Mar. Syst.*, *17*, 229–243, 1998b.
Smith, R. C., K. S. Baker, and S. E. Stammerjohn, Exploring sea ice indexes for polar ecosystem studies, *BioScience*, *48*, 83–93, 1998c.
Smith, R. C., et al., Marine ecosystem sensitivity to climate change, *BioScience*, *49*, 393–404, 1999.
Stager, J. C., and P. A. Mayewski, Abrupt early to mid-Holocene climatic transition registered at the equator and the poles, *Science*, *276*, 1834–1836, 1997.
Stammerjohn, S. E., and R. C. Smith, Opposing Southern Ocean climate patterns as revealed by trends in regional sea ice coverage, *Clim. Change*, *37*, 617–639, 1997.
Steig, E. J., E. J. Brook, J. W. C. White, C. M. Sucher, M. L. Bender, S. J. Lehman, D. L. Morse, E. D. Waddington, and G. D. Clow, Synchronous climate changes in Antarctica and the North Atlantic, *Science*, *282*, 92–95, 1998.
Taylor, F., and C. Sjunneskog, Postglacial marine diatom record of the Palmer Deep, Antarctic Peninsula (ODP Leg 178, Site 1098), 2, Diatom assemblages, *Paleoceanography*, *17*, 10.1029/2000PA000564, in press, 2002.
Thompson, L. G., D. A. Peel, E. Mosley-Thompson, R. Mulvaney, J. Dai, P. N. Lin, M. E. Davis, and C. F. Raymond, Climate since AD 1510 on Dyer Plateau, Antarctic Peninsula: Evidence for recent climate change, *Ann. Glaciol.*, *20*, 420–426, 1994.
White, W. B., and R. G. Peterson, An Antarctic circumpolar wave in surface pressure, wind temperature, and sea-ice extent, *Nature*, *380*, 699–702, 1996.
Wigley, T. M. L., and P. M. Kelly, Holocene climatic change, ^{14}C wiggles and variations in solar irradiance, *Philos. Trans. R. Soc. London*, *330*, 547–560, 1990.
Yoon, H. I., B.-K. Park, Y. Kim, and D. Kim, Glaciomarine sedimentation and its paleoceanographic implications along the fjord margins in the South Shetland Islands, Antarctica during the last 6000 years, *Palaeogeogr. Palaeoclimatol. Palaeoecol.*, *157*, 189–211, 2000.

J. P. Kennett and A. E. Shevenell, Department of Geological Sciences and the Marine Science Institute, University of California, Santa Barbara, CA 93106, USA. (amelia@geosci.geol.ucsb.edu)